

**Density Peaking in the JFT-2M Tokamak Plasma
with Counter Neutral Beam Injection**

K. Ida, S.-I. Itoh, K. Itoh, S. Hidekuma
Y. Miura, H. Kawashima, M. Mori, T. Matsuda
N. Suzuki, H. Tamai, T. Yamauchi
and JFT-2M Group

(Received - Apr. 1, 1991)

NIFS-83

May 1991

This report was prepared as a preprint of work performed as a collaboration research of the National Institute for Fusion Science (NIFS) of Japan. This document is intended for information only and for future publication in a journal after some rearrangements of its contents.

Inquiries about copyright and reproduction should be addressed to the Research Information Center, National Institute for Fusion Science, Nagoya 464-01, Japan.

Density Peaking in the JFT-2M Tokamak Plasma
with Counter Neutral Beam Injection

K.Ida, S.-I.Itoh, K.Itoh, S.Hidekuma
National Institute for Fusion Science
Nagoya, 464-01, Japan

Y.Miura, H.Kawashima, M.Mori, T.Matsuda,
N.Suzuki, H.Tamai, T.Yamauchi
and JFT-2M Group
Japan Atomic Energy Research Institute
Naka-machi, Naka-gun, Ibaraki, 311-01, Japan

A significant particle pinch and reduction of the effective thermal diffusivity are observed after switching the neutral beam direction from co- to counter- injection in the JFT-2M tokamak. A time delay in the occurrence of density peaking to that of plasma rotation is found. This shows that the particle pinch is related to the profile of the electric field as determined by the plasma rotation profile. The measured particle flux shows qualitative agreement with the theoretically-predicted inward pinch.

Keywords: Peaked density profile, plasma rotation,
radial electric field, improved confinement, inward pinch,
counter Neutral Beam Injection, JFT-2M tokamak

The improvement of core confinement has been found to be associated with peaked electron density in various tokamak discharges. Many approaches to produce the peaked electron density profile have been found. Central fueling with pellet injection in ohmic discharge have extended the linear ohmic confinement regime to higher densities in Alcator-C¹). Pellet injection is also been effective in additionally heated plasmas. Beam fueling in low density operation produced a peaked density plasma with a significantly high temperature in TFTR²). A rapid decrease of electron density at the plasma edge can also produce peaked density profiles as demonstrated by reducing the gas puff (IOC-mode) in ASDEX³), or as observed at the transition from the H-mode to the L-mode under helium beam injection (improved L-mode) in JFT-2M⁴). Recently, counter(ctr)-neutral beam(NB) heating⁵) has been found to produce peaked density profiles. An enhancement of the energy confinement time τ_E with this density peaking under ctr-NBI heating has been reported in ASDEX⁵⁻⁷). The relation between the momentum confinement and energy confinement has been discussed in TFTR and JET^{8, 9}). However, the mechanism of density peaking with ctr-NB has not been clarified yet.

Density peaking with ctr-NBI is not due to the change of the beam fueling profile nor to the decrease of edge density. It is related to the change of the direction of the toroidal rotation and resultant radial electric field. We study the

influence of the injection direction by switching injection directions with respect to the current from co to counter. In this paper, we present the radial electric field and particle flux profiles for the plasma in the JFT-2M tokamak with flat (co-NBI) and peaked (ctr-NBI) density profiles. We study the difference in the temporal evolution of toroidal velocity and density peaking. It is found that the change in toroidal rotation velocity takes place first, when the velocity reached certain value, then the density starts peaking (ctr-phase) or reduces peaking (co-phase). This delay time is larger than energy confinement time. Comparison with the inward particle pinch model¹⁰⁾ is also discussed.

JFT-2M is a tokamak with major radius $R=1.3$ m and minor radius $a=0.34$ m. It has two tangential neutral beams, one is in parallel (co-injection) and the other is anti-parallel (counter-injection) to the plasma current. The profile of radial electric field was found affected by changing the direction of momentum input from co- to ctr- injection¹¹⁾. We interchange the neutral beams during the discharge to study the response of the electric field and particle flux, keeping the absorbed power constant. These series of experiments were done under the conditions of a toroidal field B_t of 1.3T, a plasma current I_p of 240kA and an NBI power of 0.5-0.6 MW at an injection energy of 32 keV. The profiles of the toroidal rotation velocity, v_ϕ , and ion temperature T_i , are measured with multi-channel charge exchange spectroscopy (CXS)¹²⁾ every 16.6 ms. The time evolution of electron temperature T_e is measured with soft X-ray PHA with

50ms integration. Profiles of electron temperature and density n_e are obtained with a 13-channel Thomson scattering system. The line-averaged density \bar{n}_e is given by a 3-channel FIR laser interferometer, and the total stored energy W_p is estimated by diamagnetic loops.

Figure 1 shows a typical example of the change in various plasma parameters; v_ϕ at $\rho=0.15$ (ρ being the averaged minor radius), line averaged electron density \bar{n}_e at $\rho=0.25$, total stored energy W_p , central electron temperature $T_e(0)$, central and volume-averaged ion temperature $T_i(0)$ and $\langle T_i \rangle$, and peaking parameters of electron density and ion temperature profile, $n_e(0)/\langle n_e \rangle$, $T_i(0)/\langle T_i \rangle$, for a discharge where the neutral beam directions are interchanged. (Notation $\langle \rangle$ indicates the volume average.) The co-NBI is achieved from 550ms to 750ms with an absorbed power P_{abs} of 0.49 MW, and ctr-NBI is on from 750ms to 950ms with $P_{abs} = 0.56$ MW. The toroidal rotation velocity v_ϕ at $\rho=0.15$ changes within 30 ms after the onset of counter injection, and the electric field, which is evaluated from the ion force balance, changes within an MHD time scale in response to the change of rotation. Both \bar{n}_e and W_p increase in the phase of ctr-injection, the energy confinement time being 18 ms for the co-NBI phase and 24 ms for the ctr-NBI phase. The total stored energy W_p saturates at $t > 850$ ms, and starts to decrease after $t = 900$ ms. The saturation and decrease of the total stored energy at later times in the ctr-NBI phase are correlated with the decrease of the electron temperature as shown in

Fig.1(c). The central electron temperature remains constant for 100 ms after ctr-NBI is initiated until impurities accumulate at the plasma center and the radiated power at the plasma center becomes comparable to the input power. On the other hand, the central ion temperature dips for 30 ms while plasma rotation is suppressed by the interchange of the neutral beam. However, the volume averaged ion temperature does not show the dip just after the beam direction is interchanged. This dip of central ion temperature is due to the flattening of its profile, which is illustrated in Fig.1 (d). The central ion temperature starts to increase as the plasma rotation increases its velocity in the opposite direction, and becomes higher than the electron temperature 100 ms after the ctr-NBI is turned on. This fact shows the significant improvement of ion heat transport during ctr-NBI, because the beam energy is mainly deposited to electrons. The peaking parameter of electron density profile ($n_e(0)/\langle n_e \rangle$) is estimated from the ratio of two line-averaged densities measured at $\rho = 0.25$ and $\rho = 0.6$, assuming a parabolic-shaped profile raised to some power. This estimate agrees with the results from the electron density profile measured with Thomson scattering (TS) in an initial phase, and gives a slightly lower estimation at the later time. The density profile becomes flatter in the co-injection phase compared to the Ohmic phase, and shows peaking in the counter-injection phase. On the other hand, the peaking parameter of ion temperature derived from CXS measurements becomes peaked in the co-injection phase compared to the Ohmic phase. It shows

flattening when the toroidal rotation velocity changes its direction after the interchange of the NBI direction from co- to ctr-injection; this short flattening is not observed in the density profiles.

From these observations we study the relationship between confinement improvement and the peakings of T_i and n_e . The changes in stored energy and density peaking $n_e(0)/\langle n_e \rangle$ correlate, phenomenologically, with the direction of the NBI. However $T_i(0)/\langle T_i \rangle$ does not depend on it in the same manner. This quantity depends on the sign of the velocity but depends more strongly on the absolute value of v_ϕ . On the contrary, the increment of $n_e(0)/\langle n_e \rangle$ takes place only in the case of counter-injection. These observations show there is no one-to-one correspondence between peakedness of electron density and ion temperature. Note that the absolute value of T_i is larger in CTR phase than in CO phase.

There is the remaining question whether the peaking of the electron density profile is caused due to the momentum input in the ctr-direction or due to the change of toroidal rotation (or radial electric field). To answer this question, the time delay between the evolution of $n_e(0)/\langle n_e \rangle$ and $v_\phi(0)$ is studied in two types of discharges: the NBI is switched from co- to ctr- in one discharge, and from ctr- to co-injection in the other discharge to investigate the response of particle transport to the plasma rotation. Figure 2 shows the time evolution of the density peaking parameter as a function of central toroidal rotation

velocity. Each point represents an observation, spaced 16.6ms apart. The change in peaking parameter appears 30 - 80 ms after the interchange of the NBI direction. The time delay in the change of the peaking parameter is experimentally observed to be much longer than the slowing down time of the beam ions. From this observation, it is clear that the density peaking is not related to the direction of momentum input but to the toroidal rotation velocity itself. It is also noted that the change of $n_e(0)/\langle n_e \rangle$ occurs when v_ϕ reaches a certain critical velocity.

Since significant peaking of the electron density is observed in the counter phase, some inward particle pinch should exist. A pinch model associated with electric field shear has been proposed. Here we compare the profiles of the particle pinch flux and radial electric field with the model¹⁰⁾. To calculate the radial electric field ($\partial\Phi/\partial r$) profiles, the profiles of toroidal rotation velocity (v_ϕ), ion temperature and electron density are measured at 690 ms and 890 ms for the discharge shown in Fig.1. The radial electric field profile is given by the momentum balance equation¹³⁾;

$$e v_\phi B_\theta = -T_i \left(\frac{\partial \ln p_i}{\partial r} - (\beta_1, g_{2,i}) \frac{\partial \ln T_i}{\partial r} + \frac{e}{T_i} \frac{\partial \Phi}{\partial r} \right), \quad (1)$$

where $(\beta_1, g_{2,i})$ are numerical coefficients depending on the collisionality regime. Particle fluxes are estimated from the time evolution of electron density profiles $\partial n_e / \partial t(r)$ measured with Thomson scattering and the FIR laser interferometer, and

particle deposition profiles due to the neutral beam. The profiles of toroidal rotation velocity, radial electric field and transport-related quantities are summarized in Fig.3 for the discharge of Fig.1. The rate of change in electron density $\partial n_e / \partial t$ during ctr-NBI is estimated as an average over the time period from 750ms to 890ms. This change in electron density is comparable to the particle source provided by NBI fast ions at $p > 0.5$; However, it is much larger than the source near the plasma center ($p < 0.5$) as shown in Fig.3(c). The increase of electron density is not due to the reduction of the particle diffusion but due to the inward particle flow. In order to concentrate our study on the differences in particle flow between the co- and ctr- phases, we do not take into account of the particle source from the plasma edge which shows no change between co- and ctr- phase near the plasma center. In the co-NBI phase, the density profile is in steady state, and there is no $\partial n_e / \partial t$. The outward particle flux during the co-NBI phase is balanced by particle deposition of co-NBI, while the particle flux in the ctr-phase is determined from particle deposition of ctr-NBI and $\partial n_e / \partial t$. The estimated particle flux is positive (outward) in co-NBI phase, and it becomes negative (inward) for the counter-NBI phase. The magnitude of the inward particle flux in the counter phase is comparable to that of the outward particle flux in the co-NBI phase. Sawtooth oscillations with the inversion radius of $a/3$ exist both in the co- and ctr-NBI

phases. The period of the sawteeth is 10 ms in co-NBI and 20 ms in ctr-NBI phase. Although each sawtooth produces an outward flow at the crash, this effect is masked by the time averaging in estimating $\partial n_e / \partial t$. It is noted that the inward flow estimated here is an underestimation due to sawteeth effect.

Improvement of energy confinement with ctr-NBI compared to co-NBI is clear from figure 1, since the ion temperature and electron density increased with similar input powers. The energy flow is obtained from beam power deposition and energy transfer from, or to, electrons. The energy exchange between ions and electrons is reversed in the counter-injection phase. In order to avoid the error of the energy exchange between ions and electrons, we introduce an effective thermal conductivity defined by $q_{\text{cond}} / (n_e \partial T_e / \partial r + n_i \partial T_i / \partial r)$ as a measure of improvement in energy confinement. The effective conductivity is reduced in counter-NBI phase by a factor of three, although the reduction of thermal diffusivity near the plasma edge is 30 - 50% as shown in Fig3(f). This reduction is consistent with the increase of total stored energy confinement. The inward heat convection due to inward particle pinch is much smaller than the conduction. The majority of the change in χ_{eff} is due to the conductive part not the convective part, as shown in Fig.3(e). However it remains a question whether the improvement of ion confinement, reduction of effective χ_{eff} is due to a reduction of conductivity or an additional heat pinch.

Even though the measurements have some ambiguity, it is

worthwhile to compare with the particle flux predicted by the inward pinch model. According to the model, the flux is written as^{12,14)}

$$\Gamma = -D \left(\frac{\partial n}{\partial r} + \frac{\alpha \partial T}{\partial r} \frac{n}{T} - \frac{e E_r}{T} n + \frac{\omega B_t}{(m/r) T} n \right), \quad (2)$$

where D is a diffusion coefficient, α is a numerical coefficient of order unity, ω and m/r denote the frequency and wave number of the mode for a drift-type micro-turbulence. Using measured density and temperature gradients and radial electric field profiles along with the assumption of $\omega=0$, we estimate the particle flux with the model for various value of D diffusion coefficients. The flux is proportional to D according to the model. The diffusion coefficients of the order of 0.01 - 0.1 m^2/s are consistent with particle fluxes which match the experimental values. Also noted is that the shape of Γ is recovered except edge regions. This value of D may be smaller than the measured values of $D(0)$ in the improved mode of ASDEX¹⁵⁾. Since we have no direct measurements of the diffusion coefficient and fluctuation spectrum in the core region for these discharges, and the effect of the sawtooth oscillations on particle transport is not included due to poor time resolution, more precise measurements of the inward flow are needed to make a quantitative comparison with the model.

In conclusion, the peaking of the density profile is observed 30-100 ms after the neutral beam direction is switched

from co- to counter-, driven by an electric field profile changing from a positive to a negative direction. The inward pinch flux to produce this peaked electron density shows qualitative agreement with the inward pinch model.

The authors thank Dr. K.Tani (JAERI) for making available to us the numerical codes of neutral beam deposition power and Dr. K. McCormick (IPP Garching) for useful comments and critical reading of the manuscript. They also thank Dr. H.Sanuki (NIFS) for discussion, and Drs. H.Maeda (JAERI) and Y.Hamada (NIFS) for their continuous encouragement.

References

- 1) M.Greenwald, D.Gwinn, S.Milora, J.Paker, R.Parker, S.Wolfe, et al., **53** 352 (1984).
- 2) J.D.Strachan et al., Phys. Rev. Lett. **58** (1987) 1004.
- 3) F.X.Soldner, E.R.Muller, F.Wagner, et al. Phys. Rev. Lett. **61** 1105 (1988).
- 4) M.Mori, N.Suzuki, et al., Nucl. Fusion. **28** 1891 (1988).
- 5) O.Gehre, O.Gruber, H.D.Murmann, D.E.Roberts, F.Wagner, et al., Phys. Rev. Lett. **60** 1502 (1988).
- 6) O.Gruber, F.Wagner, M.Kaufmann, K.Lackner, H.Murmann, D.E.Roberts, C.Wellmer, *in Controlled Fusion and Plasma*

- Heating, 1988*, (European physical Society, Petit-Lancy, Switzerland, 1988), Vol.12B, Part.I, p.23.
- 7) V.Mertens, et al., *Plasma Phys. Contl. Fusion* **32**, 965 (1990).
 - 8) S. Scott, et al., *Phys. Rev. Lett.* **64**, 531 (1990).
 - 9) J. A. Snipes, et al., *Nucl. Fusion* **30**, 205 (1990).
 - 10) S.-I. Itoh, *J. Phys. Soc. Jpn.* **59** (1990) 3431.
 - 11) G.A.Hallock, J.Mathew, W.C.Jennings, R.L.Hickok, *Phys. Rev. Lett.* **56** 1248 (1986).
 - 12) K.Ida and S.Hidekuma, *Rev. Sci. Instrum.* **60** 867 (1989).
 - 13) F.L.Hinton and R.D.Hazeltine *Rev.Mod. Phys.* **48** 239 (1976).
 - 14) R. D. Hazeltine, S. M. Mahajan, D. A. Hichcock, *Phys. Fluids* **24**, 1164 (1981).
 - 15) O.Gehre, G.Fussmann, K.W.Gentle, K.Krieger, in *Controlled Fusion and Plasma Heating, 1988* , (European physical Society, Petit-Lancy, Switzerland, 1988), Vol.12B , Part.I, p.167.

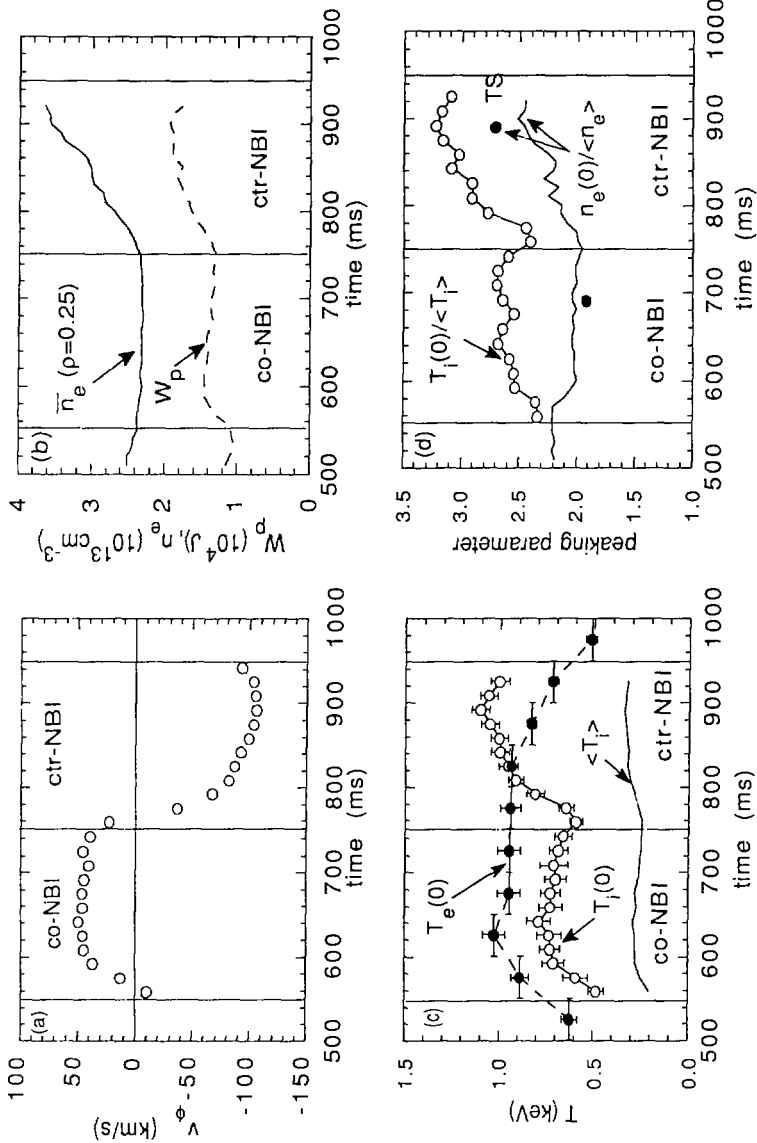


Figure 1

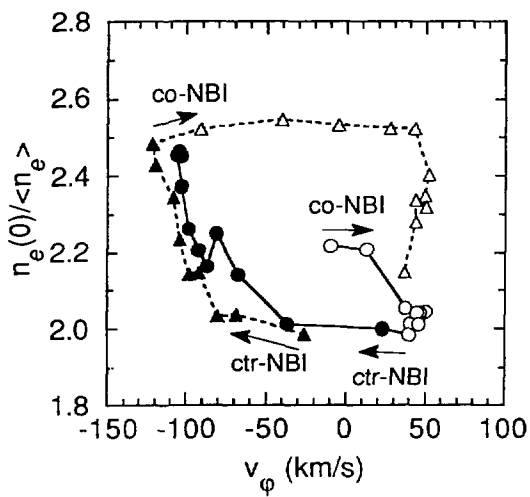


Figure 2

K. Ida et al.

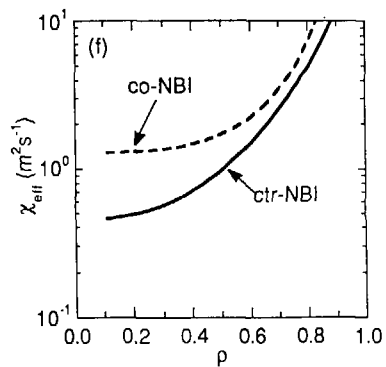
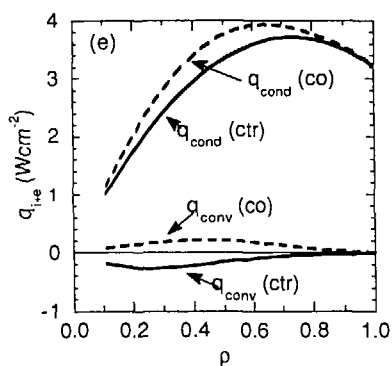
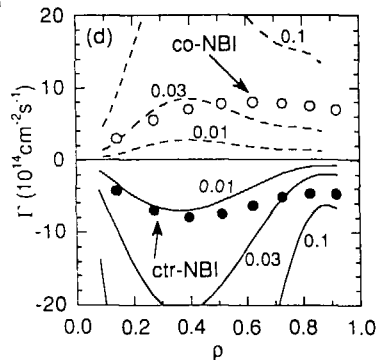
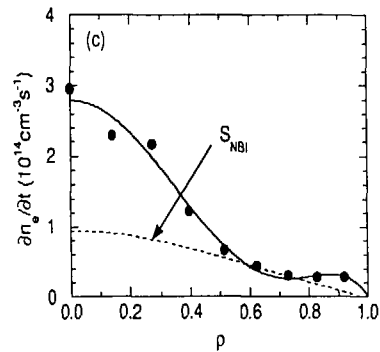
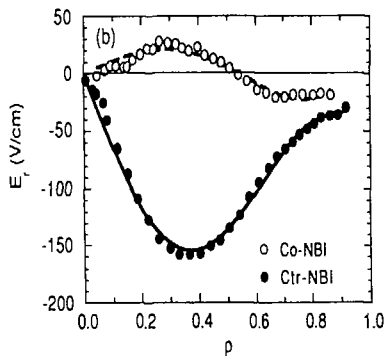
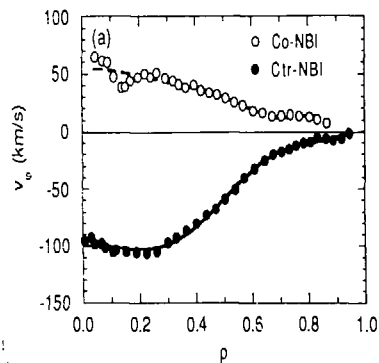


Figure 3

Recent Issues of NIFS Series

- NIFS-33 S.-I. Itoh, *Anomalous Viscosity due to Drift Wave Turbulence* ; June 1990
- NIFS-34 K. Hamamatsu, A. Fukuyama, S.-I. Itoh, K. Itoh and M. Azumi, *RF Helicity Injection and Current Drive* ; July 1990
- NIFS-35 M. Sasao, H. Yamaoka, M. Wada and J. Fujita, *Direct Extraction of a Na- Beam from a Sodium Plasma* ; July 1990
- NIFS-36 N. Ueda, S.-I. Itoh, M. Tanaka and K. Itoh, *A Design Method of Divertor in Tokamak Reactors* Aug. 1990
- NIFS-37 J. Todoroki, *Theory of Longitudinal Adiabatic Invariant in the Helical Torus*; Aug. 1990
- NIFS 38 S.-I. Itoh and K. Itoh, *Modelling of Improved Confinements - Peaked Profile Modes and H-Mode-* ; Sep. 1990
- NIFS-39 O. Kaneko, S. Kubo, K. Nishimura, T. Syoji, M. Hosokawa, K. Ida, H. Idei, H. Iguchi, K. Matsuoka, S. Morita, N. Noda, S. Okamura, T. Ozaki, A. Sagara, H. Sanuki, C. Takahashi, Y. Takeiri, Y. Takita, K. Tsuzuki, H. Yamada, T. Amano, A. Ando, M. Fujiwara, K. Hanatani, A. Karita, T. Kohmoto, A. Komori, K. Masai, T. Morisaki, O. Motojima, N. Nakajima, Y. Oka, M. Okamoto, S. Sobhanian and J. Todoroki, *Confinement Characteristics of High Power Heated Plasma in CHS*; Sep. 1990
- NIFS-40 K. Toi, Y. Hamada, K. Kawahata, T. Watari, A. Ando, K. Ida, S. Morita, R. Kumazawa, Y. Oka, K. Masai, M. Sakamoto, K. Adati, R. Akiyama, S. Hidekuma, S. Hirokura, O. Kaneko, A. Karita, T. Kawamoto, Y. Kawasumi, M. Kojima, T. Kuroda, K. Narihara, Y. Ogawa, K. Ohkubo, S. Okajima, T. Ozaki, M. Sasao, K. Sato, K.N. Sato, T. Seki, F. Shimo, H. Takahashi, S. Tanahashi, Y. Taniguchi and T. Tsuzuki, *Study of Limiter H- and IOC- Modes by Control of Edge Magnetic Shear and Gas Puffing in the JIPP T-III Tokamak*; Sep. 1990
- NIFS 41 K. Ida, K. Itoh, S.-I. Itoh, S. Hidekuma and JIPP T-III & CHS Group. *Comparison of Toroidal/Poloidal Rotation in CHS Heliotron/Torsatron and JIPP T-III Tokamak*; Sep. 1990
- NIFS 42 T. Watari, R. Kumazawa, T. Seki, A. Ando, Y. Oka, O. Kaneko, K. Adati, R. Ando, T. Aoki, R. Akiyama, Y. Hamada, S. Hidekuma, S. Hirokura, E. Kako, A. Karita, K. Kawahata, T. Kawamoto, Y. Kawasumi, S. Kitagawa, Y. Kitoh, M. Kojima, T. Kuroda, K. Masai, S. Morita, K. Narihara, Y. Ogawa, K. Ohkubo, S. Okajima, T. Ozaki, M. Sakamoto, M. Sasao, K. Sato, K.N. Sato, F. Shinbo, H. Takahashi, S. Tanahashi, Y. Taniguchi, K. Toi,

- T.Tsuzuki, Y.Takase, K.Yoshioka, S.Kinoshita, M.Abe, H.Fukumoto, K.Takeuchi, T.Okazaki and M.Ohtuka, *Application of Intermediate Frequency Range Fast Wave to JIPP T-IIU and HT-2 Plasma*; Sep. 1990
- NIFS-43 K.Yamazaki, N.Ohyabu, M.Okamoto, T.Amano, J.Todoroki, Y.Ogawa, N.Nakajima, H.Akao, M.Asao, J.Fujita, Y.Hamada, T.Hayashi, T.Kamimura, H.Kaneko, T.Kuroda, S.Morimoto, N.Noda, T.Obiki, H.Sanuki, T.Sato, T.Satow, M.Wakatani, T.Watanabe, J.Yamamoto, O.Motojima, M.Fujiwara, A.Iiyoshi and LHD Design Group, *Physics Studies on Helical Confinement Configurations with $l=2$ Continuous Coil Systems*; Sep. 1990
- NIFS-44 T.Hayashi, A.Takei, N.Ohyabu, T.Sato, M.Wakatani, H.Sugama, M.Yagi, K.Watanabe, B.G.Hong and W.Horton, *Equilibrium Beta Limit and Anomalous Transport Studies of Helical Systems*; Sep. 1990
- NIFS-45 R.Horiuchi, T.Sato, and M.Tanaka, *Three-Dimensional Particle Simulation Study on Stabilization of the FRC Tilting Instability*; Sep. 1990
- NIFS-46 K.Kusano, T.Tamano and T. Sato, *Simulation Study of Nonlinear Dynamics in Reversed-Field Pinch Configuration*; Sep. 1990
- NIFS-47 Yoshi H.Ichikawa, *Solitons and Chaos in Plasma*; Sep. 1990
- NIFS-48 T.Seki, R.Kumazawa, Y.Takase, A.Fukuyama, T.Watari, A.Ando, Y.Oka, O.Kaneko, K.Adachi, R.Akiyama, R.Ando, T.Aoki, Y.Hamada, S.Hidekuma, S.Hirokura, K.Ida, K.Itoh, S.-I.Itoh, E.Kako, A. Karita, K.Kawahata, T.Kawamoto, Y.Kawasumi, S.Kitagawa, Y.Kitoh, M.Kojima, T.Kuroda, K.Masai, S.Morita, K.Narihara, Y.Ogawa, K.Ohkubo, S.Okajima, T.Ozaki, M.Sakamoto, M.Sasao, K.Sato, K.N.Sato, F.Shinbo, H.Takahashi, S.Tanahashi, Y.Taniguchi, K.Toi and T.Tsuzuki, *Application of Intermediate Frequency Range Fast Wave to JIPP T-IIU Plasma*; Sep.1990
- NIFS-49 A.Kageyama, K.Watanabe and T.Sato, *Global Simulation of the Magnetosphere with a Long Tail: The Formation and Ejection of Plasmoids*; Sep.1990
- NIFS-50 S.Koide, *3-Dimensional Simulation of Dynamo Effect of Reversed Field Pinch*; Sep. 1990
- NIFS-51 O.Motojima, K. Akaishi, M.Asao, K.Fuji, J.Fujita, T.Hino, Y.Hamada, H.Kaneko, S.Kitagawa, Y.Kubota, T.Kuroda, T.Mito, S.Morimoto, N.Noda, Y.Ogawa, I.Ohtake, N.Ohyabu, A.Sagara, T. Satow, K.Takahata, M.Takao, S.Tanahashi, T.Tsuzuki, S.Yamada, J.Yamamoto, K.Yamazaki, N.Yanagi, H.Yonezu, M.Fujiwara, A.Iiyoshi and LHD Design Group, *Engineering Design Study of Superconducting Large Helical Device*; Sep. 1990

- NIFS-52 T.Sato, R.Horiuchi, K. Watanabe, T. Hayashi and K.Kusano, *Self-Organizing Magnetohydrodynamic Plasma*; Sep. 1990
- NIFS-53 M.Okamoto and N.Nakajima, *Bootstrap Currents in Stellarators and Tokamaks*; Sep. 1990
- NIFS-54 K.Itoh and S.-i.Itoh, *Peaked-Density Profile Mode and Improved Confinement in Helical Systems*; Oct. 1990
- NIFS-55 Y.Ueda, T.Enomoto and H.B.Stewart, *Chaotic Transients and Fractal Structures Governing Coupled Swing Dynamics*; Oct. 1990
- NIFS 56 H.B.Stewart and Y.Ueda, *Catastrophes with Indeterminate Outcome*; Oct. 1990
- NIFS-57 S.-i.Itoh, H.Maeda and Y.Miura, *Improved Modes and the Evaluation of Confinement Improvement*; Oct. 1990
- NIFS-58 H.Maeda and S.-i.Itoh, *The Significance of Medium- or Small-size Devices in Fusion Research*; Oct. 1990
- NIFS-59 A.Fukuyama, S.-i.Itoh, K.Itoh, K.Hamamatsu, V.S.Chan, S.C.Chiu, R.L.Miller and T.Ohkawa, *Nonresonant Current Drive by RF Helicity Injection*; Oct. 1990
- NIFS-60 K.Iida, H.Yamada, H.Iguchi, S.Hidekuma, H.Sanuki, K.Yamazaki and CHS Group, *Electric Field Profile of CHS Heliotron/Torsatron Plasma with Tangential Neutral Beam Injection*; Oct. 1990
- NIFS-61 T.Yabe and H.Hoshino, *Two- and Three-Dimensional Behavior of Rayleigh-Taylor and Kelvin-Helmholtz Instabilities*; Oct. 1990
- NIFS-62 H.B. Stewart, *Application of Fixed Point Theory to Chaotic Attractors of Forced Oscillators*; Nov. 1990
- NIFS-63 K.Konn., M.Mituhashi, Yoshi H.Ichikawa, *Soliton on Thin Vortex Filament*; Dec. 1990
- NIFS-64 K.Itoh, S.-i.Itoh and A.Fukuyama, *Impact of Improved Confinement on Fusion Research*; Dec. 1990
- NIFS -65 A.Fukuyama, S.-i.Itoh and K. Itoh, *A Consistency Analysis on the Tokamak Reactor Plasmas*; Dec. 1990
- NIFS-66 K.Itoh, H. Sanuki, S.-i. Itoh and K. Tani, *Effect of Radial Electric Field on α -Particle Loss in Tokamaks*; Dec. 1990
- NIFS 67 K.Sato and F.Miyawaki, *Effects of a Nonuniform Open Magnetic Field on the Plasma Presheath*; Jan.1991
- NIFS-68 K.Itoh and S.-i.Itoh, *On Relation between Local Transport Coefficient and Global Confinement Scaling Law*; Jan. 1991

- NIFS-69 T.Kato, K.Masai, T.Fujimoto, F.Koike, E.Källne, E.S.Marmor and J.E.Rice, *He-like Spectra Through Charge Exchange Processes in Tokamak Plasmas*; Jan.1991
- NIFS-70 K. Ida, H. Yamada, H. Iguchi, K. Itoh and CHS Group, *Observation of Parallel Viscosity in the CHS Heliotron/Torsatron* ; Jan.1991
- NIFS-71 H. Kaneko, *Spectral Analysis of the Heliotron Field with the Toroidal Harmonic Function in a Study of the Structure of Built-in Divertor* ; Jan. 1991
- NIFS-72 S. -I. Itoh, H. Sanuki and K. Itoh, *Effect of Electric Field Inhomogeneities on Drift Wave Instabilities and Anomalous Transport* ; Jan. 1991
- NIFS-73 Y.Nomura, Yoshi.H.Ichikawa and W.Horton, *Stabilities of Regular Motion in the Relativistic Standard Map*; Feb. 1991
- NIFS-74 T.Yamagishi, *Electrostatic Drift Mode in Toroidal Plasma with Minority Energetic Particles*, Feb. 1991
- NIFS-75 T.Yamagishi, *Effect of Energetic Particle Distribution on Bounce Resonance Excitation of the Ideal Ballooning Mode*, Feb. 1991
- NIFS-76 T.Hayashi, A.Takei, N.Ohyabu and T.Sato, *Suppression of Magnetic Surface Breaking by Simple Extra Coils in Finite Beta Equilibrium of Helical System*; Feb. 1991
- NIFS-77 N.Ohyabu, *High Temperature Divertor Plasma Operation*; Feb. 1991
- NIFS-78 K.Kusano, F.Yamano and T.Sato, *Simulation Study of Toroidal Phase-Locking Mechanism in Reversed-Field Pinch Plasma*; Feb 1991
- NIFS-79 K.Nagasaki, K.Itoh and S-I.Itoh, *Model of Divertor Biasing and Control of Scrape-off Layer and Divertor Plasmas*; Feb. 1991
- NIFS-80 K.Nagasaki and K.Itoh, *Decay Process of a Magnetic Island by Forced Reconnection*; Mar.1991
- NIFS-81 K.Takahata, N.Yanagi, T.Mito, J.Yamamoto, O.Motojima and LHD Design Group, K.Nakamoto, S.Mizukami, K.Kitamura, Y.Wachi, H.Shinohara, K.Yamamoto, M.Shibui, T.Uchida and K.Nakayama, *Design and Fabrication of Forced-Flow Coils as R&D Program for Large Helical Device*; Mar.1991
- NIFS-82 T.Aoki and T.Yabe, *Multi-dimensional Cubic Interpolation for ICF Hydrodynamics Simulation*; Apr.1991